AIRCRAFT MODELLING FOR NONLINEAR AND ROBUST CONTROL DESIGN AND ANALYSIS

Andrés Marcos[†], Jean Marc Biannic[◇], Matthieu Jeanneau[*], Declan G. Bates[†], Ian Postlethwaite[†]

[†]*Dept. of Engineering, University of Leicester, University Road, Leicester, LE1 7RH, U.K., {– –, dgb3, ixp} @le.ac.uk*
[◇]*Dept. of Flight Control Systems and Dynamics, ONERA, Toulouse, 31055, France, biannic@onera.fr*
[*]*Airbus, 316 Route de Bayonne, 31300, Toulouse, France, Matthieu.Jeanneau@airbus.com*

Abstract:
In this paper an application of an exact nonlinear symbolic LFT modelling approach to an On-Ground Airbus aircraft is shown. The modelling approach used combines the natural modularity and clarity of presentation from LFT modelling with the ease of manipulation from symbolic algebra. It results in an exact nonlinear symbolic LFT that represents an ideal starting point to perform subsequent simplifications and assumptions to finally transform the model into an approximated symbolic LFT ready for design and analysis.

Keywords: LFT, On-Ground Aircraft Motion, Nonlinear Symbolic Modelling

Notation

θ_{NWS}	Nose wheel angle, rad
$\Pi = [x\ y\ z]^T$	Earth-based aircraft position, m
$\Omega = [p\ q\ r]^T$	Angular velocities, rad/s
$\Xi = [\phi\ \theta\ \psi]^T$	Euler angles, rad
$F = [F_x\ F_y\ F_z]^T$	Body-axes total forces, Nwt
$F_a = [X\ Y\ Z]^T$	Aerodynamic forces $= \frac{1}{2}\rho S V^2 C_{axis}$, Nwt
$M = [M_x\ M_y\ M_z]^T$	Body-axes total moments, Nwt*m
$V = [V_x\ V_y\ V_z]^T$	Velocity vector at c.g., m/s
$BT_{MLG_{L/R}}$	Braking torque Right/Left Main-Landing-Gear
ISV_{NWS}	Servovalve steering control current, mA
ISV_{brk}	Servovalve braking control current, mA
$Lxyz_{cmp}$	Relative distance to c.g. along xyz-axes, m
$N1_c$	Engine fan speed target, r.p.m.
$Tn_{L/R}$	Right/Left engine thrust, Nwt
s_{ang}/c_{ang}	sine/cosine of angle *ang*, rad

1. INTRODUCTION

Over the last twenty years, a paradigm shift in the modelling of dynamic systems has occurred with the introduction of modern robust control theory and its associated modelling framework, the linear fractional transformation (LFT) (Packard, A. and Doyle, J., 1993). Commonly, LFTs are used to represent a nonlinear system as an approximated linear system formed by a constant M matrix in linear feedback with a structured matrix Δ which contains the system uncertainty (the so-called 'M-Δ' form). The linear approximation allows the application of linear control and analysis techniques while the explicit use of an uncertainty matrix imbues the designs and analyses with robustness properties. Two drawbacks of standard usage of LFT modelling are: its restriction to linear systems, which means there is an inherent loss of modelling fidelity that may result in conservatism, and a lack of modelling control and flexibility (which arises from the standard use of computational linearization).

More recently, many industries are making significant efforts to develop and apply nonlinear synthesis and analysis techniques - see for example, the work reported in (Fielding, C. *et al.*, 2002) for recent progress in the aerospace industry. One approach to this prob-

⋆ Andrés Marcos is now at the Advanced Projects Division in Deimos Space S.L., Ronda de Poniente 19, 28760, Madrid, Spain. Email: andres.marcos@deimos-space.com This research was supported thanks to EPSRC-UK under research grant $GR/S61874/01$.

lem which has been very successful in practice is to extend traditional linear design and analysis methods to address nonlinear problems. This is the basis of modern synthesis and analysis techniques such as gain scheduling (Leith, D.J. and Leithead, W.E., 2000), linear parameter varying (LPV) control (Becker, G. and Packard, A, 1994), and integral quadratic constraints (Megretski, A. and Rantzer, A., 1995) among others. It is noted that many of these techniques work with LFT-like models. Thus, it is advantageous to develop a systematic nonlinear modelling framework, based on LFT representations, that offers flexibility and modularity. Furthermore, the modelling approach should result in a nonlinear LFT that can be fit easily to the different (linear and nonlinear) design and analysis techniques.

In this paper an aircraft modelling example is described that uses such a nonlinear modelling framework. The aircraft application is a high-fidelity nonlinear On-Ground Airbus model and the purpose of the model is to allow nonlinear and linear clearance analysis and design techniques for on-ground control.

2. MODELLING APPROACH

The modelling approach used is the nonlinear symbolic LFT framework from (Marcos, A. *et al.*, 2005*b*). The basic idea is to use symbolic techniques to represent the ordinary differential equations (ODEs) – which define the nonlinear system – as an exact nonlinear symbolic LFT where the structured Δ matrix contains the nonlinear, time-varying and uncertain terms as symbolic parameters.

Assume the class of nonlinear systems considered are defined by the following ODEs:

$$\dot{x} = f(x,u) = f_1(x)\,x + f_2(x)\,u + f_3(x) \qquad (1)$$
$$y = g(x,u) = g_1(x)\,x + g_2(x)\,u + g_3(x) \qquad (2)$$

where the nonlinear functions $f_i(x), g_i(x)$ are given by a polynomial mix of analytic expressions and tabular data. The basic steps of the modelling approach are:

1. Represent the ODEs as a nonlinear state-space 2×2 block matrix using, if needed, fictitious signals $u_f = 1\ \forall\ t$ to include those nonlinear terms not affine on the inputs u or the states x:

$$\begin{bmatrix}\dot{x}\\ y\end{bmatrix} = \left[\begin{array}{c|cc} f_1(x) & f_2(x) & f_3(x)\\ \hline g_1(x) & g_2(x) & g_3(x)\end{array}\right]\begin{bmatrix}x\\ u\\ u_f\end{bmatrix} \qquad (3)$$

2. Declare as symbolic parameters ρ_k all the uncertain, nonlinear and/or time-varying terms as well as those physical parameters that can vary with operational condition (e.g. discrete switches). The guiding principle proposed at this stage is *to select everything that is not a known constant c_j as a symbolic parameter* ρ_k:

$$f_i(x) = f_i(\rho_1^{n1},\ldots,\rho_k^{nk},c_1,\ldots,c_j) \qquad (4)$$

   where $n1, n2, \ldots, nk$ indicate the number of repetitions for each parameter.
3. Transform the resulting nonlinear symbolic 2×2 matrix into a nonlinear symbolic LFT where all the symbolic parameters (and their repetitions) are included in the $\Delta(\rho)$ matrix. This step is automatically carried out using available exact reduced-order LFT modelling software: **symtreed** (Magni, J.F., 2004), **LHT** (Marcos, A. *et al.*, 2005*a*), and **ETD** (Hecker, S. *et al.*, 2005) for this particular project.

   Note that the three steps above result in an LFT representation which is identical to the original nonlinear system given by equations (1-2).
4. Taking advantage of the diagonal structure of $\Delta(\rho)$ arising from the previous LFT modelling process it is possible now to carry out: *i*) simplifications, *ii*) model reduction, *iii*) approximations, and *iv*) uncertainty characterization, in order to obtain a manageable LFT model for design and analysis. Furthermore, the modularity afforded by the symbolic LFT allows easy updating of the model if any assumption needs to be corrected.

3. ON-GROUND AIRCRAFT MODEL

The nonlinear model characterizes the aircraft on-ground dynamics of a representative Airbus transport with two engines (Jeanneau, M., 2004) during on-ground rolling (i.e. taxi and after-touchdown). The open-loop nonlinear model can be represented by three main blocks of ODEs, see Figure 1.

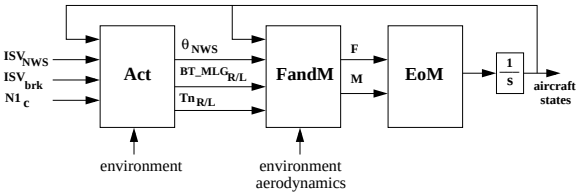

Fig. 1. On-Ground Aircraft Model Diagram.

The equations of motion block, **EoM**, is generic for all aircraft (on-ground and airborne) and comprises the twelve standard aircraft degrees of freedom (Stevens, B. and Lewis, F., 1992). The inputs are the total forces and moments (F and M) and the outputs are the linear and angular accelerations ($\dot{V}$ and $\dot{\Omega}$) and the kinematic ($\dot{\Xi}$) and navigation ($\dot{\Pi}$) derivatives of the states.

$$\begin{bmatrix}\dot{V}\\ \dot{\Omega}\\ \dot{\Xi}\\ \dot{\Pi}\end{bmatrix} = \begin{bmatrix}\dfrac{F}{m} - \Omega\wedge V\\ I^{-1}(M - \Omega\wedge(I\cdot\Omega))\\ T_{HB}\cdot\Omega\\ T_{BE}\cdot V\end{bmatrix} \qquad (5)$$

where T_{HB} and T_{BE} are transformation matrices from local-horizon to body-axes and from body-axes to Earth-frame respectively, and I is the inertial matrix.

The total forces and moments **FandM** block has as inputs the aircraft states x, environment *env* and aerodynamic *aero* data, and the actuator inputs (θ_{NWS}, $BT_{MLG_{R/L}}$, $Tn_{R/L}$):

$$\begin{bmatrix}F_x\\ F_y\\ F_z\end{bmatrix} = F_a + \begin{bmatrix}-mgs_\theta\\ mgs_\phi c_\theta\\ mgc_\phi c_\theta\end{bmatrix} + \begin{bmatrix}\Sigma Tn_{R/L}\\ 0\\ 0\end{bmatrix} + [T_{WB}\cdot F_w] \qquad (6)$$

T_{WB} is a transformation matrix from wheel-frame to body-frame, and F_w represents the nose wheel and landing gear contributions, which model the nonlinear interactions between the shock absorbers and the runway friction. These interactions are condensed in lateral and longitudinal forces due to wheel slip, rolling drag and braking forces (Bakker, E. and Pacejka, H.B., 1989; Barnes, A.G. and Yager, T.J, 1998; Clot, J. *et al.*, 1998). The moments are given by, $M = F\cdot L$, where L is the proper moment-arm.

The actuator block **Act**, transforms the avionics commands from the pilot/on-ground-autopilot (ISV_{NWS}, ISV_{brk} and $N1_c$) into the FandM actuator inputs. This block is formed by three subsystems: nose-wheel steering system, braking system and engine model. The latter is modelled by a first quasi-steady stage followed by a dynamic model with amplitude and rate limits. The nose-wheel steering system calculates θ_{NWS} using mechanical components, servovalves and pistons models for the hydraulic components:

$$\dot{\theta}_{NWS} = K_1 \sigma_1[ISV_{NWS}] \sqrt{\frac{\sigma_2[K_2 - |\Delta P_{NWS}|\,]}{1 + K_3\,\sigma_1[ISV_{NWS}]}} \qquad (7)$$

where σ_i represent saturation functions, K_i different NWS geometric and physical constants, and ΔP_{NWS} is a nonlinear function of the pistons' pressure and θ_{NWS}. Similarly for the braking system (one equation per $_{MLG}$ boggie):

$$\dot{P}_{brk} = \frac{\beta_{brk}}{V_{brk}} \eta S_{brk}[ISV_{brk}, P_{brk}] \sqrt{\Delta P_{brk}} \qquad (8)$$

where β_{brk} is a compressibility coefficient dependent on the braking pistons' pressure difference ΔP_{brk} (which is a function of P_{brk}), V_{brk} is the piston swept volume, η is the flow coefficient, and S_{brk} is a saturation function for the servovalve switching logic.

4. EXACT NONLINEAR SYMBOLIC LFT

Using the first three steps from Section 2, an exact nonlinear symbolic LFT for each of the three main blocks is obtained. Since a full and detailed presentation of the LFT modelling process is not possible for space consideration, only a general view of the different steps is given with emphasis on the drawbacks and practical considerations incurred during the process.

4.1 EoM block

Step 1 is direct in this case due to the standard manner of writing the ODEs for an aircraft motion (i.e. affine on the states or inputs).
Step 2 we follow the symbolization rule to select 24 symbolic parameters (states, inertial coefficients and trigonometric functions) and no symbolic constants. Summing up the repetitions of the 24 "independent" parameters results in an order of 67.
Step 3 an *exact nonlinear symbolic LFT* of order 43 with 23 symbolic parameters in Δ is finally obtained. Table 1 shows the results for the three order-reduction LFT techniques before and after application of a ND numerical minimization technique (D'andrea, R. and Khatri, S., 1997), the latter also keeps the exactness of the models. All the min-ND LFT models result in the same number of repetitions for each of the 23 parameters (this is not a typical situation). Thus, any of the exact LFT models models can be chosen.

Table 1. Exact LFT for EoM block.

	no-min	**min-ND**
symtreed	53	43
LHT	44	43
ETD	51	43

General practical considerations:

- Initially, declare each physical parameter as symbolic and only group them as a new ρ if functional expression is complex, e.g. $\rho_1 = \sqrt{pq}$ but $\rho_2 \neq pq$.
- The symbolic parameters are considered 'independent' at this stage (e.g. $\rho_1 = s_\theta$, $\rho_2 = c_\theta$ and $\rho_3 = \theta$).
- The reciprocal of a parameter is considered also a parameter (e.g. $\rho_1 = m$ and $\rho_2 = m^{-1}$).
- Select carefully which parameter is extracted from a monomial, see example below.
- In general, the selected exact LFT model is that with the lowest LFT order. This might not be appropriate if step 4 of the modelling approach is to be used afterwards. For example, a better candidate could be a LFT model where some of the most repeated parameters are known to be set constant (after assumptions are applied).

Example 1. The yaw rate state derivative is given by:

$$\dot{r} = (c_8\, p - c_2\, r)\, q + c_4\, M_x + c_9\, M_z \qquad (9)$$

where c_i are inertial coefficients, p, q, r are aircraft states, and M_x, M_z are inputs. Therefore, two possible exact nonlinear 2×2 state-spaces are:

$$\dot{r} = \begin{bmatrix} c_8 q & -c_2 q \end{bmatrix} \begin{bmatrix} p \\ r \end{bmatrix} + \begin{bmatrix} c_4 & c_9 \end{bmatrix} \begin{bmatrix} M_x \\ M_z \end{bmatrix} \qquad (10)$$

$$\dot{r} = [c_8 p - c_2 r]\,[q] + \begin{bmatrix} c_4 & c_9 \end{bmatrix} \begin{bmatrix} M_x \\ M_z \end{bmatrix} \qquad (11)$$

both represent a total order of 6 but the first for 5 symbolic parameters (c_i, q) and the second for six (c_i, p, r). Thus, the first representation is better. □

4.2 FandM block

Step 1 and **Step 2** are more complex than before since F_w presents a more difficult development for the nonlinear matrix and force a larger number of symbolic declarations. The chosen number of $\rho's$ is now 27 (of which 9 are specially defined to map some quite complex functional dependencies) plus 15 symbolic constants (mostly relative distances to the aerodynamic center), see example 2. Furthermore, an indication of the complexity for this block is the fact that the input vector is augmented to include the vertical forces due to the wheels Fz_{NWS} and Fz_{MLG}. These forces are highly nonlinear and it is decided to use them as inputs due to the manner they enter the system (they are calculated in a separate block from the xy-plane forces). The total order of the nonlinear 2×2 matrix is 314 counting both the repetitions of the parameters and constants (251 for the $\rho's$ alone).

Example 2. The lateral contribution of the landing gear forces and moments are based on the calculation of the local sideslip angle for the wheels. For the particular case of the nose wheel sideslip angle β_{NWS}:

$$\beta_{NWS} = atan\left(\frac{V_y + r\, Lx_{NWS}}{V_x}\right) - \theta_{NWS} \qquad (12)$$

Choose $\rho_1 = atan(\frac{V_y + r\, Lx_{NWS}}{V_x})$ and use a fictitious input to yield the exact nonlinear state-space:

$$\beta_{NWS} = \begin{bmatrix} -1 & \rho_1 \end{bmatrix} \begin{bmatrix} \theta_{NWS} \\ u_f \end{bmatrix} \qquad (13)$$

In this manner, we can later approximate the arc-tan during step 4, see (Biannic, J.M. *et al.*, 2006). □

Step 3 Table 2 shows the orders obtained after applying the LFT modelling and ND numerical minimization techniques (the number within parentheses for the min-ND column gives the order counting only the symbolic parameters):

4.3 Act block

Step 1 and **Step 2** This block is mainly formed by saturation functions and logic switches in general

Table 2. Exact LFT for FandM block.

	no-min	min-ND
symtreed	177	134 (89)
LHT	215	180 (120)
ETD	190	139 (87)

difficult to model. Similar to example 2, saturation functions can be represented by a symbolic parameter (times the input to the saturation if needed), e.g. $sat(u) = \rho \cdot u$ where $\rho = \frac{sat(u)}{u} \forall u \neq 0$. See for example the symbolization of Equation 7:

$$\dot{\theta}_{NWS} = c_1 \rho_1 \rho_2 \rho_3 ISV_{NWS} \tag{14}$$

$$c_1 = K_1; \qquad \rho_2 = \frac{1}{\sqrt{1 + K_3\, \sigma_1}} \tag{15}$$

$$\rho_1 = \frac{\sigma_1[ISV_{NWS}]}{ISV_{NWS}}; \quad \rho_3 = \sqrt{\sigma_2[K_2 - |\Delta P_{NWS}|]} \tag{16}$$

Thus, the nonlinear symbolic parameters are defined to condense all these nonlinear functions resulting in a total of 15 $\rho's$ and 6 $c's$ (mostly geometrical information about the pistons, brakes and nose wheel). **Step 3** The corresponding orders for the exact LFT models are given in Table 3:

Table 3. Exact LFT for Act block.

	no-min	min-ND
symtreed	28	26
LHT	24	24
ETD	24	24

The three exact nonlinear LFTs with lowest order are combined and the final exact order-reduced LFT order and number of parameters are given in Table 4:

Table 4. Exact symbolic LFT.

	order	**no.** ρ	**no.** c
EoM	43	24	0
FandM	134	27	15
Act	24	15	6
total	201	61	21

5. NON-EXACT NONLINEAR SYMBOLIC LFT

Step 4 in Section 2 can be used now to reduce the order of the LFT further. However, it is noted that as these additional order reduction tools involve simplifications, model reductions and approximations, the LFT thus obtained will no longer represent an exact model of the aircraft nonlinear system.

Also, the process is now highly automatized due to the (LFT and symbolic) nature of the exact LFT model above and the use of the LFT software mentioned before.

In (Jeanneau, M., 2004) several standing simplifications and assumptions are provided since the aircraft model is intended for design and analysis of steering and speed/braking on-ground controllers:

- A.1 No inertial cross-coupling terms ($c2 = c4 = c6 = 0 \Rightarrow$ coupling of M_x and M_z dropped).
- A.2 Small-angle approximations and low speeds (less than 150 knots) $\Rightarrow$ neglect products of angles and velocity terms.
- A.3 Runway is perfectly horizontal $\Rightarrow$ the lift is quasi-constant and there are almost no variations on the vertical position of the center of gravity.
- A.4 Neglect compressibility effects of shock absorbers $\Rightarrow$ quasi-steady pitch and roll.
- A.5 bicycle model $\Rightarrow$ superimposed left and right MLGs $\Rightarrow$ two points of contact with runway.

5.1 EoM block

Using Assumptions A.1, A.2 and noting A.3 is translated as assuming that the vertical position is constant, i.e. $\dot{V}_z = V_z = 0 \Rightarrow F_z = 0$, then we obtain:

$$\begin{bmatrix} \dot{V}_x \\ \dot{V}_y \\ \dot{r} \\ \dot{\psi} \end{bmatrix} = \begin{bmatrix} 0 & V_y & m^{-1} & 0 & 0 \\ -V_x & 0 & 0 & m^{-1} & 0 \\ c_8 p & 0 & 0 & 0 & c_9 \\ \phi & 1 & 0 & 0 & 0 \end{bmatrix} \begin{bmatrix} q \\ r \\ F_x \\ F_y \\ M_z \end{bmatrix} \tag{17}$$

The corresponding non-exact LFT has an order of 8 for a total of 5 ρ's (V_x, V_y, p, ϕ, m^{-1}) and two symbolic inertial constants (c_8, c_9).

5.2 FandM block

From the previous EoM reduction we have now:

A.6 $F_z = M_x = M_y = 0$

From this EoM assumption we could largely simplify the engine and aerodynamic forces, but some of the neglected forces and moments are used internally to calculate F_w thus, the aerodynamic forces and moments F_a, M_a remain the same as before and the engine forces and moments are given by:

$$\begin{bmatrix} Fx_{eng} \\ My_{eng} \\ Mz_{eng} \end{bmatrix} = \begin{bmatrix} 1 & 1 \\ Lz_{engR} & Lz_{engL} \\ -Ly_{engR} & -Ly_{engL} \end{bmatrix} \begin{bmatrix} Tn_R \\ Tn_L \end{bmatrix} \tag{18}$$

Using assumptions A.2 and A.3, the gravity forces can be simplified: $Fx_g = Fy_g = 0$ and $Fz_g = mg$.

Now, recall that previously we had chosen the wheels' forces along the z-axis Fz_w as inputs. This design choice remains but we can reduce the wheels force and moment effects along the other two axes using assumptions A.4 and A.5. After some long and complicated algebra it is possible to represent the x/y-axes wheel forces as (these are valid for the NWS and the two MLG boggies, except that $Fx_{NWS} = 0$):

$$\begin{bmatrix} Fx_w \\ Fy_w \end{bmatrix} = \begin{bmatrix} \dfrac{wT_{MLG}(BT_{MLG_{R/L}})}{Rw} \\ G_y(Fz_w)\beta_w \dfrac{\beta opt_w^2}{\beta_w^2 + \beta opt_w^2} \end{bmatrix} \tag{19}$$

where wT_{MLG} is the main-landing-gear wheel friction function and Rw the wheel radius. G_y is a cornering gain dependent on the Fz_w inputs.

Finally, the non-exact FandM LFT orders are given in Table 5 and the number of symbolic parameters is now reduced to 19 plus 10 constants:

Table 5. Non-exact LFT for FandM block.

	no-min	min-ND
symtreed	48	41
LHT	61	45
ETD	56	47

5.3 ACT block

After a Monte Carlo analysis of the different components for the three subsystems in the *Act* block (i.e. simulations of the ρ's from the exact LFT model of the engine, nose-wheel steering and braking subsystems), we are able to reduced their complexity to linear approximations based on a subset of the symbolic parameters.

The *NWS* steering system can be approximated as:

$$\dot{\theta}_{NWS} = \bar{K}_1 ISV_{NWS} \tag{20}$$

where $\bar{K}_1$ is a non-symbolic constant. The braking systems (one per boggie) are given now by:

$$\begin{aligned}\dot{P}_{brk} =& \beta_{brk}(\bar{K}_2 + \bar{K}_3\sigma_1[P_{brk}] + \bar{K}_4\sigma_2[ISV_{brk}]) \\ =& \rho_1(\bar{K}_2 u_f + \bar{K}_3\rho_2 P_{brk} + \bar{K}_3\rho_3 ISV_{brk})\end{aligned} \tag{21}$$

where again $\bar{K}_i$ are non-symbolic constants and the symbolic parameters represent input-normalized saturations, e.g. $\rho_2 = \frac{\sigma_1[P_{brk}]}{P_{brk}}$. Note, that $P_{brk} = \frac{1}{s}\dot{P}_{brk}$ is then used to calculate the left/right braking torques, $BT_{MLG} = G_{brk}P_{brk}$ where $G_{brk} = \rho_4$ is a braking disc gain with large variations. Therefore, the braking system approximation yields 8 symbolic parameters (three in $\dot{P}_{brk}$ and one for G_{brk} –per boggie).

Finally, the engine model is (also left and right):

$$\begin{aligned}\ddot{N1} =& LUT_1^2 N1_c - LUT_1^2 N1 - 2LUT_1 LUT_2 \dot{N1} \\ =& \rho_9^2 N1_c - \rho_{10}^2 N1 - 2\rho_9\rho_{10}\dot{N1}\end{aligned} \tag{22}$$

where LUT_i are look-up tables containing the engine dynamic/static information.

Combining all the *Act* subsystems, the non-exact Act LFT models are obtained for a total of 12 symbolic parameters, see the orders in Table 6:

Table 6. Non-exact LFT for Act block.

	no-min	**min-ND**
symtreed	18	14
LHT	14	14
ETD	14	14

As before, the lowest order LFT models are combined to yield the total non-exact nonlinear LFT, see Table 7, which is now half the number of parameters and almost a third the order of the exact LFT model:

Table 7. Non-Exact symbolic LFT.

	order	**no.** ρ	**no.** c
EoM	8	5	2
FandM	41	19	10
Act	14	12	0
total	63	36	12

6. DESIGN AND ANALYSIS (DESANA) LONGITUDINAL MODEL

In this section we follow the previous process to derive an LFT model for the longitudinal motion ($\dot{V}_x$) which can be used for *des*ign and *ana*lysis (*desana* model). The force identification/approximation method used in this section arises from (Biannic, J.M. *et al.*, 2006) where the LFT modelling approach presented here is also used for the lateral/directional modelling of the on-ground aircraft.

From equations 5 and 6, the nonlinear longitudinal velocity is given by:

$$\begin{aligned}\dot{V}_x =& V_y r - V_z q + \frac{1}{m}F_x \\ F_x =& Fx_a + Fx_g + Tn_x + T_{WB}\cdot Fx_w \\ =& \hat{q}V^2(-C_x c_\alpha + C_z s_\alpha) - mgs_\theta \\ &+ \Sigma Tn - \theta_{NWS} Fy_{NWS} + \Sigma Fx_{MLG}\end{aligned} \tag{23}$$

where $\hat{q} = 0.5\rho_{air}S$ is the (constant) air density ρ_{air} and wing-surface S component of the dynamic pressure, and C_x, C_z are the stability-axes aerodynamic coefficients.

For this type of vehicle, it is possible to decouple the motion into 'pure' longitudinal and lateral/directional components:

$$\begin{aligned}\dot{V}_x^{long} =& -gs_\theta + m^{-1}\hat{q}V^2(-C_x c_\alpha + C_z s_\alpha) \\ &+ m^{-1}\Sigma Tn + m^{-1}\Sigma Fx_{MLG}\end{aligned} \tag{24}$$

$$\dot{V}_x^{lat} = V_y r - V_z q - m^{-1}\theta_{NWS} Fy_{NWS} \tag{25}$$

The lateral contribution will be used to complement the resulting $\dot{V}_x^{long}$ LFT model during simulation, thus we now focus on the LFT modeling of the latter:

$$\begin{aligned}\dot{V}_x^{long} =& -\bar{K}_1\rho_1 u_f + \bar{K}_2\bar{K}_3\rho_2(-\rho_3 + \rho_4)V \\ &+ \bar{K}_2\Sigma Tn + \bar{K}_2\Sigma Fx_{MLG}\end{aligned} \tag{26}$$

$$\bar{K}_1 = g; \qquad \bar{K}_2 = m^{-1}; \qquad \bar{K}_3 = \hat{q}; \tag{27}$$

$$\rho_1 = s_\theta; \qquad \rho_2 = V; \tag{28}$$

$$\rho_3 = C_x c_\alpha; \quad \rho_4 = C_z s_\alpha; \tag{29}$$

Note that the left/right thrust Tn and MLG Fx_{MLG} forces are inputs together with the ground speed V. The exact LFT order is four (one for each ρ).

From Section 5, we can simplify the ρ's using **i)** $\rho_3 = C_x c_\alpha \approx Cx$ and $\rho_4 = C_z s_\alpha \approx 0$ by A.2 and A.3, **ii)** $V \approx V_x = \rho_2$ due to the larger contribution of V_x, **iii)** $Fx_{MLG-R} = Fx_{MLG-L}$ by assumption A.5, and more over **iv)** $\rho_5 = Fx_{MLG} = \sigma[-4Fx_{MLG-0}V_x]$ where $Fx_{MLG-0} = \bar{K}_4$ (obtained by simulation tests):

$$\dot{V}_x^{long} = -\bar{K}_1\rho_1 u_f - \bar{K}_2(\bar{K}_3\rho_2\rho_3 V_x - \Sigma Tn - 2\rho_5 u_f) \tag{30}$$

Notice that the previous simplifications are carried out directly on the Δ symbolic matrix and do not affect the exact LFT model order (i.e. it is only required to assign the new values to the ρ's).

Furthermore, from additional simulations with different manoeuvres, it is observed that $\rho_1 = s_\theta \approx \bar{K}_5 r$ (with r as a new input). This require the use of the nested LFT substitution from (Marcos, A. *et al.*, 2005*b*) and results in a non-exact LFT with input $u = [Tn_R \;\; Tn_L \;\; r]'$ and state $x = V_x$:

$$\begin{aligned}\dot{V}_x^{long} =& [-\bar{K}_{2,3}\rho_2\rho_3]V_x + [\bar{K}_2 \;\; \bar{K}_2 \;\; -\bar{K}_{1,5}]\,u \\ y =& [-4\bar{K}_4]V_x\end{aligned} \tag{31}$$

where $\rho_5 (= sat[y]\,)$ has been transformed into a deadzone nonlinearity considered as a new symbolic parameter, i.e. $\rho_5 = y - dz[y] = (1+\rho_6)y$. This is easily posed as an LFT and combined with that from equation 31 to obtain a LFT with three ρ's and order 3.

Next, a requirement for the usability of the model is to assume several parametric uncertainties:

- U.1 Each engine thrust has a common 10 % multiplicative uncertainty, $\hat{Tn} = (1 + 0.1Tn_\Delta)Tn$.
- U.2 The aerodynamic coefficient has 25 % uncertainty, $\hat{Cx} = (1 + 0.25Cx_\Delta)Cx$.
- U.3 There are x-axis wind effects, $[-\bar{K}_{2,3}\rho_2\rho_3]Vw_x$.

These new requirements are easily transformed into new LFTs (with $\rho_7 = Tn_\Delta$ and $\rho_8 = Cx_\Delta$) that can be combined with the previous one to get the final non-exact LFT longitudinal model (of order 4):

$$\begin{aligned}\dot{V}_x^{long} =& [A]V_x + [\bar{K}_2\rho_7 \;\; \bar{K}_2\rho_7 \;\; -\bar{K}_{1,5} \;\; A]\,\bar{u} \\ y =& [4\bar{K}_4]V_x\end{aligned} \tag{32}$$

where $A = -\bar{K}_{2,3}\rho_{2,3,8}$, $\bar{u} = [Tn_R \;\; Tn_L \;\; r \;\; Vw_x]'$, and the symbolic matrix is $\Delta = diag\{\Delta_{NL}, \Delta_{LTV}, \Delta_{LTI}\}$ with:

$$\Delta_{NL} = \rho_6 = dz[y] \cdot I_1 \quad (33)$$
$$\Delta_{LTV} = \rho_2 = V_x \cdot I_1 \quad (34)$$
$$\Delta_{LTI} = diag\{\rho_7, \rho_8\} = diag\{Tn_\Delta \cdot I_1, Cx_\Delta \cdot I_1\} \quad (35)$$

with the ρ's normalized to ± 1 (direct since the matrix Δ is diagonal and its normalization does not introduce an increment in the LFT order).

7. SIMULATION RESULTS

In this section, the exact and non-exact LFT models from Sections 4 and 5 together with the longitudinal desana non-exact LFT model from Section 6 are compared to the original nonlinear model from Section 3.

The validity of the LFT models was tested using a set of standard on-ground manoeuvres. Figure 2 shows the time responses of all the models using a 80 % $N1_c$ step at t=2 seconds (reduced to 70 % at t=25 sec) followed by a $\pm$ 5 degrees doublet in the pedals.

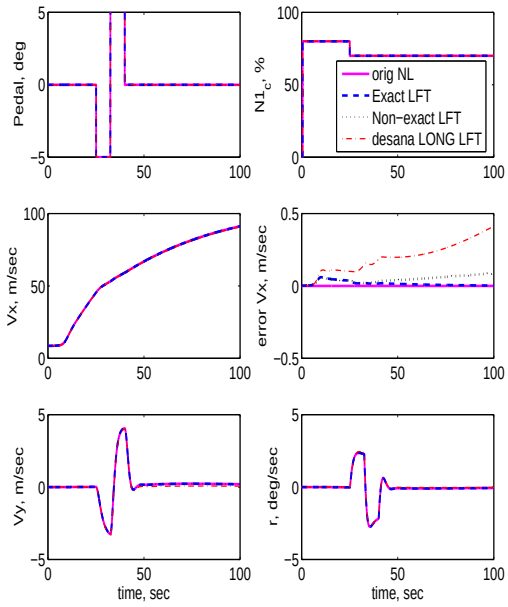

Fig. 2. Time response of nonlinear / exact LFT / non-exact LFT / long. non-exact desana LFT models.

The responses shown are the pedal and $N1_c$ commands (top two plots), the longitudinal velocity and its error with respect to the nonlinear model (second row), and the lateral velocity and yaw rate (bottom plot). Note that the responses of the nonlinear (solid line), exact LFT (dashed line) and non-exact LFT (dotted line) are almost indistinguishable, see the V_x error plot. Furthermore, the longitudinal desana LFT model (dashed dotted line) is also very close (only a maximum of 0.5 m/s of error when $V_x \approx 100 m/s$).

In conclusion, the desana LFT model is of a size (LFT order) and number of parameters that is very manageable by current robust techniques. Also, since the fidelity of the model is very good (measured by time simulations), then the model can be used for robust or nonlinear design/analysis with a high level of confidence.

8. CONCLUSIONS

In this paper, an application of a nonlinear modelling framework to a complex, nonlinear aircraft on-ground model has been shown. The modelling approach is quite automatized due to the availability of LFT modelling software and to the ease of manipulations of LFTs. The responses of the resulting LFT models compare favourably with the original nonlinear model.

REFERENCES

Bakker, E. and Pacejka, H.B. (1989). A New Tyre Model with an Application in Vehicle Dynamics Studies. Technical Report 890087. SAE.

Barnes, A.G. and Yager, T.J (1998). Enhancement of Aircraft Ground Handling Simulation Capability. Technical Report AGARDograph 333. AGARD.

Becker, G. and Packard, A (1994). Robust Performance of Linear Parametrically Varying Systems Using Parametrically Dependent Linear Dynamic Feedback. *Systems and Control Letters* **23**(3), 205–215.

Biannic, J.M., Marcos, A., Jeanneau, M. and Roos, C. (2006). Nonlinear simplified LFT modelling of an aircraft on ground. In: *submitted to IEEE Conference on Control Applications*. Munich, Germany.

Clot, J., Falipou, J., Sentenac,T., Pebayle, P., Lorenzi, F. and Marchant, S. (1998). Systeme d'alarme et de securite active pour la conduite automobile. Technical Report 98441. LAAS-CNRS.

D'andrea, R. and Khatri, S. (1997). Kalman decomposition of linear fractional transformation representations and minimality. In: *American Control Conference*. Alburquerque, NM. pp. 3557–3561.

Fielding, C., Varga, A., Bennani, S. and Selier, M., Eds.) (2002). *Advanced Techniques for Clearance of Flight Control Laws*. number 283 In: *Lecture Notes in Control and Information Sciences*. Springer Verlag.

Hecker, S., Varga, A. and Magni, J.F. (2005). Enhanced LFR-Toolbox for Matlab. *Aerospace Science and Technology*.

Jeanneau, M. (2004). Description of aircraft ground dynamics. Technical Report RP0412731. GARTEUR. Airbus proprietary.

Leith, D.J. and Leithead, W.E. (2000). Survey of Gain-Scheduling analysis and Design. *International Journal of Control* **73**(11), 1001–1025.

Magni, J.F. (2004). Linear Fractional Representation Toolbox Modelling, Order Reduction, Gain Scheduling. Technical Report TR 6/08162 DCSD. ONERA, Systems Control and Flight Dynamics Department. Toulouse, France.

Marcos, A., Bates, D.G. and Postlethwaite, I. (2005*a*). A Multivariate Polynomial Matrix Order-Reduction Algorithm for Linear Fractional Transformation Modeling. In: *IFAC World Congress*. Praga, CH.

Marcos, A., Bates, D.G. and Postlethwaite, I. (2005*b*). Exact Nonlinear Modeling using Symbolic Linear Fractional Transformations. In: *IFAC World Congress*. Praga, CH.

Megretski, A. and Rantzer, A. (1995). System analysis via integral quadratic constraints: Part i. Technical Report LUTD2/TFRT-7531-SE. Department of Automatic Control, Lund Institute of Technology.

Packard, A. and Doyle, J. (1993). The complex structured singular value. *Automatica* **29**(1), 71–109.

Stevens, B. and Lewis, F. (1992). *Aircraft Control and Simulation*. 2 ed.. John Wiley & Sons, Inc.